

Transverse Vibration and Stability Analysis of Circular Plate Subjected to Follower Force and Thermal Load

Yongqiang Yang^{1,2} and Zhongmin Wang^{3,*}

¹School of Mechanical and Precision Instrument Engineering, Xi'an University of Technology, 710048, Xi'an, China.

²College of Mechanical & Electrical Engineering, Shaanxi University of Science & Technology, 710021, Xi'an, China.

³School of Civil Engineering and Architecture, Xi'an University of Technology, 710048, Xi'an, China.

*Corresponding Author: Zhongmin Wang. Email: wangzhongm@xaut.edu.cn.

Abstract: Transverse vibration and stability analysis of circular plate subjected to follower force and thermal load are analyzed. Based on the thin plate theory in involving the variable temperature, the differential equation of transverse vibration for the axisymmetric circular plate subjected to follower force and thermal load is established. Then, the differential equation of vibration and corresponding boundary conditions are discretized by the differential quadrature method. Meanwhile, the generalized eigenvalue under three different boundary conditions are calculated. In this case, the change curve of the first order dimensionless complex frequency of the circular plate subjected to the follower force in the different conditions with the variable temperature coefficient and temperature load is analyzed. The stability and corresponding critical loads of the circular plate subjected to follower force and thermal load with simply supported edge, clamped edge and free edge are discussed. The results provide theoretical basis for improving the dynamic stability of the circular plate.

Keywords: Circular plate; transverse vibration; follower force; thermal load, differential quadrature method; stability

1 Introduction

The transverse vibration of the circular plate has played an important part in many engineering systems, such as friction clutches, circular saws, disk brakes, and so on. Some research work has been performed on the circular plate. Bauer and Eidel [1] studied the transverse vibration of the circular plate by Galerkin method, and analyzed the effects of angular speed on the natural frequency and dynamic stability. Khorasany and Hutton [2] discussed the linear vibration behavior of the rotating plate by the modal expansion method. Gupta et al. [3] utilized Rayleigh-Ritz method to calculate the deflections of the first two modes in orthotropic viscoelastic circular plates, and discussed the effect of nonhomogeneous value and taper coefficient on transverse vibration. Wang et al. [4] analyzed the change of the complex frequencies of the rotating circular plate under three boundary conditions with the change of the angular speed by the differential quadrature method.

All of the researches mentioned above are carried out in the constant temperature field, but in actual engineering applications, the temperature is not constant which needs to be taken into consideration. The variable temperature will affect the transverse vibration and stability of the circular plate inevitably, which has been attracted some researchers' attention, and did some corresponding research. For example, Gupta [5] studied free vibration of a non-homogeneous visco-elastic circular plate with linearly varying thickness and subjected to a linear temperature load by Rayleigh-Ritz's method. Sepahi et al. [6] analyzed the effect of variable temperature on large deflection of FGM plate by the differential quadrature method. Shu and Zhan [7] used Galerkin method to discuss the nonlinear thermoelastic vibration of circular plate

with clamped edge. Sun et al. [8,9] analyzed the thermoelastic coupling vibration of micro-circular plates, and discussed the effect of different temperatures on the thermal bending moments and vibration amplitude. Hao [10] analyzed the vibration of circular thin-plate micrometer and nanometer electromechanical exciters under the heat-elastic damping.

All of these references did not take the effects of the followed force in the circular plate into consideration. In fact, a considerable research work had been done on the vibration of rectangular plates subjected to the followed force. Adali [11] analyzed and compared the stability of non-conservative and conservative rectangular plate. Leipholz and Pfenndt [12] used the Galerkin theory to analyze the transverse vibration of a rectangular plate subjected to the follower force and in the boundary condition of free edge, and discussed the critical load of rectangular plate. Guo et al. [13] investigated the stability of the moving thermoelastic coupling rectangular plate subjected to uniformly distributed tangential follower force, and analyzed the effects of the thermoelastic coupling factor and the speed on the stability and critical load of the plate. Wang et al. [14] studied the dynamic stability of the rectangular plates subjected to the uniformly distributed tangential follower force. Zuo and Shreyer [15] investigated the vibration and instability regions of the plate with simply supported edge and subjected to the fixed and follower force. However, the research on the follower force of the circular plate is not so much. Hochlenert [16] studied the vibration problem of circular plate caused by the frictional follower load in the brake system. Mottershead and Chanr [17] analyzed the flutter instability of the circular plate under the frictional follower load. Wang et al. [18] investigated the relationship between the complex frequencies and the load of the circular plate with simple supported edge and the clamped edge. Up to now, few papers have been reported on the transverse vibration and stability problems for the circular plate subjected to the follower force and thermal load.

Therefore, the aim of this paper is to establish the transverse vibration differential equation of the circular plate subjected to the follower force and thermal load. The eigenequation is obtained by the differential quadrature method, and the dimensionless complex frequencies of the circular plate are calculated. The relation curves between the follower force and the complex frequency of the circular plate with variable temperature are obtained, the effects of the follower force, the variable temperature coefficient and the temperature load on the transverse vibration and stability of the circular plate are analyzed.

2 Differential Equation of Motion

2.1 Differential Equation of Transverse Vibration with Variable Temperature

Fig. 1 shows an axisymmetric circular plate subjected to the follower force q and the variable temperature T . R and h are the radius and thickness in the polar coordinate, respectively

As shown in Fig. 2, the temperature T of the circular plate along r-direction is as follows:

$$T(r)=T_0+Kr \tag{1}$$

where $K = \frac{T_R - T_0}{R}$, $T_0 = T(0)$, $T_R = T(R)$.

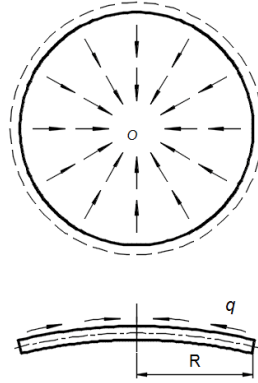


Figure 1: Schematic diagram for an axisymmetric circular plate subjected to the follower force

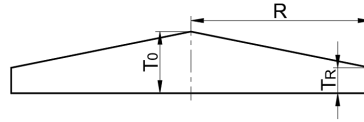


Figure 2: Temperature field of the axisymmetric circular plate

The strain-displacement relation of the circular plate can be given by

$$\begin{cases} \varepsilon_r = \frac{\partial u_r}{\partial r} = -z \frac{\partial^2 w}{\partial r^2} \\ \varepsilon_\theta = \frac{u_r}{r} = -\frac{z}{r} \frac{\partial w}{\partial r} \end{cases} \quad (2)$$

where u_r is the displacement field components along the r axis, z is the rotation axis, and $w = w(r, t)$ is the transverse displacement.

The governing equation of transverse motion is

$$D \left(\frac{\partial^4 w}{\partial r^4} + \frac{2}{r} \frac{\partial^3 w}{\partial r^3} - \frac{1}{r^2} \frac{\partial^2 w}{\partial r^2} + \frac{1}{r^3} \frac{\partial w}{\partial r} \right) + \frac{E\alpha}{1-\mu} \nabla^2 M_T + \rho h \frac{\partial^2 w}{\partial t^2} - N_r \frac{\partial^2 w}{\partial r^2} - N_\theta \frac{1}{r} \frac{\partial w}{\partial r} = 0 \quad (3)$$

where $D = \frac{Eh^3}{12(1-\mu^2)}$ is the flexural rigidity, μ is Poisson's ratio, E is elastic modulus, α is the linear thermal expansion coefficient, ρ is the density of materials, N_r and N_θ are normal in-plane forces,

$M_T = \int_{-\frac{h}{2}}^{\frac{h}{2}} Tz dz$ is the thermal moment.

N_r and N_θ are given by

$$\begin{cases} N_r = h\sigma_r \\ N_\theta = h\sigma_\theta \end{cases} \quad (4)$$

The normal forces in the plate is given by the equations of equilibrium

$$\frac{\partial N_r}{\partial r} + \frac{N_r - N_\theta}{r} - q = 0 \quad (5)$$

The relations of the strain-displacement and in-plane force with the variable temperature T may be written as

$$\begin{cases} \varepsilon_r = \frac{1}{Eh}(N_r - \mu N_\theta) + \alpha T \\ \varepsilon_\theta = \frac{1}{Eh}(N_\theta - \mu N_r) + \alpha T \end{cases} \quad (6)$$

The strain compatibility equation is obtained

$$\varepsilon_r = \frac{\partial(r\varepsilon_\theta)}{\partial r} \quad (7)$$

The following equation is derived by using Eqs. (5)-(7)

$$r^2 \frac{\partial^2 N_r}{\partial r^2} + 3r \frac{\partial N_r}{\partial r} - (2 + \mu)qr + E\alpha hr \frac{dT}{dr} = 0 \quad (8)$$

From Eq. (8), the solution of N_r can be obtained as

$$N_r = \frac{1}{2}(2 + \mu)qr - \frac{1}{2}E\alpha hT + \frac{1}{2} \frac{1}{r^2} \int \left[-(2 + \mu)q + E\alpha h \frac{dT}{dr} \right] r^2 dr + A + \frac{B}{r^2} \quad (9)$$

Substituting Eq. (1) into Eq. (9) results in:

$$N_r = \frac{1}{3}(2 + \mu)qr - \frac{1}{3}E\alpha hKr - \frac{1}{2}E\alpha hT_0 + A + \frac{B}{r^2} \quad (10)$$

where A and B are integral constants. Since stress components in the center of plate are limited, $B = 0$.

Based on Eqs. (2) and (6), u_r can be obtained as

$$u_r = \frac{r}{Eh}(N_\theta - \mu N_r) + \alpha Tr \quad (11)$$

Substituting N_θ of Eq. (5) into Eq. (11) results in

$$u_r = \frac{r}{Eh} \left[r \frac{\partial N_r}{\partial r} + (1 - \mu)N_r - qr \right] + \alpha Tr \quad (12)$$

The boundary conditions of clamped edge and simply supported edge are given by:

$$u_r|_{r=R} = 0 \quad (13)$$

Substituting Eq. (10) into Eq. (12) and solving it with respect to the above boundary condition yields

$$A = -\frac{1}{3}(1 + \mu)qR + Eh\alpha \left(\frac{1}{2}T_0 - \frac{1}{3} \frac{1 + \mu}{1 - \mu} RK - \frac{1}{1 - \mu} T_0 \right) \quad (14)$$

Substituting Eq. (14) into Eq. (10) and based on Eq. (5) results in (clamped edge and simply supported edge)

$$\begin{cases} N_r = \frac{1}{3}q[(2 + \mu)r - (1 + \mu)R] - E\alpha h \left[\frac{1}{3}K \left(\frac{1 + \mu}{1 - \mu} R + r \right) + \frac{T_0}{1 - \mu} \right] \\ N_\theta = \frac{1}{3}q[(1 + 2\mu)r - (1 + \mu)R] - E\alpha h \left[\frac{1}{3}K \left(\frac{1 + \mu}{1 - \mu} R + 2r \right) + \frac{T_0}{1 - \mu} \right] \end{cases} \quad (15)$$

The boundary condition of free edge is given by

$$\sigma_r|_{r=R} = 0 \quad (16)$$

Based on Eqs. (4), (5), (10) and (16), N_r and N_θ are given by in the boundary condition of free edge

$$\begin{cases} N_r = \frac{1}{3}q(2+\mu)(r-R) - \frac{1}{3}E\alpha hK(r-R) \\ N_\theta = \frac{1}{3}q(2+\mu)(2r-R) - \frac{1}{3}E\alpha hK(2r-R) - rq \end{cases} \quad (17)$$

2.2 Dimensionless Vibration Differential Equation and Dimensionless Boundary Conditions

The following dimensionless quantities are introduced as follows

$$\begin{aligned} \bar{r} = \frac{r}{R}, \quad \bar{w} = \frac{w}{h}, \quad \bar{z} = \frac{z}{h}, \quad c = \frac{R}{h}, \quad \bar{T} = \frac{T}{T_0}, \quad \tau = \frac{th}{R^2} \sqrt{\frac{E}{12\rho(1-\mu^2)}}, \quad \lambda = 12\alpha(1-\mu^2)c^2T_0, \quad Q = 12\frac{(1-\mu^2)}{E}c^3q, \\ g = \frac{T_R - T_0}{T_0} = \frac{K}{T_0}R \end{aligned} \quad (18)$$

Substituting Eq. (18) into Eq. (3), we can get the dimensionless forms

$$\left(\frac{\partial^4 \bar{w}}{\partial \bar{r}^4} + \frac{2}{\bar{r}} \frac{\partial^3 \bar{w}}{\partial \bar{r}^3} - \frac{1}{\bar{r}^2} \frac{\partial^2 \bar{w}}{\partial \bar{r}^2} + \frac{1}{\bar{r}^3} \frac{\partial \bar{w}}{\partial \bar{r}}\right) + A_1 \nabla^2 \bar{M}_T + \frac{\partial^2 \bar{w}}{\partial \tau^2} - N_1 \frac{\partial^2 \bar{w}}{\partial \bar{r}^2} - N_2 \frac{1}{\bar{r}} \frac{\partial \bar{w}}{\partial \bar{r}} = 0 \quad (19)$$

where $\bar{M}_T = \int_{-1/2}^{1/2} \bar{T} \bar{z} d\bar{z}$, $A_1 = 12\alpha(1+\mu)c^2T_0$.

For simply supported edge and clamped edge

$$\begin{cases} N_1 = \frac{1}{3}Q[(2+\mu)\bar{r} - (1+\mu)] - \left[\frac{1}{3}\lambda g\left(\frac{1+\mu}{1-\mu} + \bar{r}\right)\right] - \frac{\lambda}{1-\mu} \\ N_2 = \frac{1}{3}Q[(1+2\mu)\bar{r} - (1+\mu)] - \left[\frac{1}{3}\lambda g\left(\frac{1+\mu}{1-\mu} + 2\bar{r}\right)\right] - \frac{\lambda}{1-\mu} \end{cases} \quad (20)$$

For the free edge

$$\begin{cases} N_1 = \frac{1}{3}[Q(2+\mu)(\bar{r}-1) - \lambda g(\bar{r}-1)] \\ N_2 = \frac{1}{3}\left[Q(2+\mu)(2\bar{r}-1) - \frac{3\bar{r}}{2+\mu} - \lambda g(2\bar{r}-1)\right] \end{cases} \quad (21)$$

The solution of Eq. (19) is assumed in this form

$$\bar{w}(\bar{r}, \tau) = W(\bar{r})e^{j\omega\tau} \quad (22)$$

where ω denotes the dimensionless complex frequency of the circular plate.

Considering that the change of temperature along z-direction is ignored, the thermal moment $\bar{M}_T = 0$. Substituting Eq. (22) into Eq. (19), the differential equation of the circular plate is obtained as

$$\left(\frac{d^4 W}{d\bar{r}^4} + \frac{2}{\bar{r}} \frac{d^3 W}{d\bar{r}^3} - \frac{1}{\bar{r}^2} \frac{d^2 W}{d\bar{r}^2} + \frac{1}{\bar{r}^3} \frac{dW}{d\bar{r}}\right) - N_1 \frac{d^2 W}{d\bar{r}^2} - N_2 \frac{1}{\bar{r}} \frac{dW}{d\bar{r}} - \omega^2 W = 0 \quad (23)$$

Considering the edge of the plate is placed at a constant temperature, the three dimensionless boundary conditions are given as follows:

(1) Simply supported edge

$$\begin{cases} W|_{\bar{r}=1} = 0 \\ \left(\frac{d^2 W}{d\bar{r}^2} + \mu \frac{1}{\bar{r}} \frac{dW}{d\bar{r}}\right)|_{\bar{r}=1} = 0 \end{cases} \quad (24)$$

(2) Clamped edge

$$\begin{cases} W|_{\bar{r}=1} = 0 \\ \frac{dW}{d\bar{r}}|_{\bar{r}=1} = 0 \end{cases} \quad (25)$$

(3) Free edge

$$\begin{cases} \left(\frac{d^2W}{d\bar{r}^2} + \mu \frac{1}{\bar{r}} \frac{dW}{d\bar{r}}\right)|_{\bar{r}=1} = 0 \\ \left(\frac{d^3W}{d\bar{r}^3} + \frac{1}{\bar{r}} \frac{d^2W}{d\bar{r}^2} - \frac{1}{\bar{r}^2} \frac{dW}{d\bar{r}}\right)|_{\bar{r}=1} = 0 \end{cases} \quad (26)$$

The dimensionless boundary conditions of the center of the plate are given as follows:

$$\begin{cases} \frac{dW}{d\bar{r}}|_{\bar{r}=0} = 0 \\ \lim_{\bar{r} \rightarrow 0} \left(\frac{d^3W}{d\bar{r}^3} + \frac{1}{\bar{r}} \frac{d^2W}{d\bar{r}^2} - \frac{1}{\bar{r}^2} \frac{dW}{d\bar{r}}\right) = 0 \end{cases} \quad (27)$$

3 Discretization Method

The differential quadrature method (DQM)19-24 is employed to solve Eq. (23). The radial direction of the circular plate is divided into N nonuniform nodes, the δ method is adopted to treat the boundary conditions. The nodes are calculated by the following formula 24.

$$\bar{r}_1 = 0, \bar{r}_2 = \delta, \bar{r}_{N-1} = 1 - \delta, \bar{r}_N = 1, \bar{r}_i = \frac{1}{2} \left(1 - \cos \frac{(i-2)\pi}{N-3}\right) \quad (i = 3, 4, \dots, N-2) \quad (28)$$

Based on the Lagrange interpolation polynomial, the weight coefficients of the first derivative $A_{ij}^{(1)}$ is obtained

$$A_{ij}^{(1)} = \begin{cases} \frac{\prod_{k=1, k \neq i, j}^N (x_i - x_k)}{\prod_{k=1, k \neq j}^N (x_j - x_k)} & (i, j = 1, 2, \dots, N; i \neq j) \\ \sum_{k=1, k \neq i}^N \frac{1}{(x_i - x_k)} & (i, j = 1, 2, \dots, N; i = j) \end{cases} \quad (29)$$

The weight coefficients of the second, third and fourth derivatives can be expressed by matrix multiplication as follows:

$$\begin{cases} A_{ij}^{(2)} = \sum_{k=1}^N A_{ik}^{(1)} A_{kj}^{(1)} \\ A_{ij}^{(3)} = \sum_{k=1}^N A_{ik}^{(2)} A_{kj}^{(1)} \\ A_{ij}^{(4)} = \sum_{k=1}^N A_{ik}^{(3)} A_{kj}^{(1)} \end{cases} \quad (i, j = 1, 2, \dots, N) \quad (30)$$

Eq. (23) can be discretized into the following form by DQM

$$\left(\sum_{k=1}^N A_{ik}^{(4)} W_k + \frac{2}{r_i} \sum_{k=1}^N A_{ik}^{(3)} W_k - \frac{1}{r_i^2} \sum_{k=1}^N A_{ik}^{(2)} W_k + \frac{1}{r_i^3} \sum_{k=1}^N A_{ik}^{(1)} W_k \right) - N_{1i} \sum_{k=1}^N A_{ik}^{(2)} W_k - N_{2i} \frac{1}{r_i} \sum_{k=1}^N A_{ik}^{(1)} W_k - \omega^2 W_i = 0 \quad (31)$$

The differential quadrature forms of boundary conditions (24), (25) and (26) can be expressed as follows, respectively

(1) Simply supported edge

$$\begin{cases} W_N = 0 \\ \sum_{k=1}^N A_{(N-1)k}^{(2)} W_k + \mu \frac{1}{r_{(N-1)}} \sum_{k=1}^N A_{(N-1)k}^{(1)} W_k = 0 \end{cases} \quad (32)$$

(2) Clamped edge

$$\begin{cases} W_N = 0 \\ \sum_{k=1}^N A_{(N-1)k}^{(1)} W_k = 0 \end{cases} \quad (33)$$

(3) Free edge

$$\begin{cases} \sum_{k=1}^N A_{Nk}^{(2)} W_k + \mu \frac{1}{r_N} \sum_{k=1}^N A_{Nk}^{(1)} W_k = 0 \\ \sum_{k=1}^N A_{(N-1)k}^{(3)} W_k + \frac{1}{r_{(N-1)}} \sum_{k=1}^N A_{(N-1)k}^{(2)} W_k - \frac{1}{r_{(N-1)}^2} \sum_{k=1}^N A_{(N-1)k}^{(1)} W_k = 0 \end{cases} \quad (34)$$

The discretization of Eq. (27) can be expressed in the following form

$$\begin{cases} \sum_{k=1}^N A_{1k}^{(1)} W_k = 0 \\ \sum_{k=1}^N A_{2k}^{(3)} W_k + \frac{1}{r_2} \sum_{k=1}^N A_{2k}^{(2)} W_k - \frac{1}{r_2^2} \sum_{k=1}^N A_{2k}^{(1)} W_k = 0 \end{cases} \quad (35)$$

Eq. (31), the boundary condition (35) and the one of the boundary conditions (32)-(34) can be written in the matrix form

$$(\omega^2 [I] + [K]) \{W\} = 0 \quad (36)$$

where the matrix $[K]$ and $[I]$ involve the follower force Q , the variable temperature coefficient g and the temperature load λ . Eq. (36) is a generalized eigenvalue equation of the circular plate subjected to the follower force and thermal load.

4 Results and Discussions

In order to verify the present formulation and method, the transverse vibration equation is reduced and the results are compared with those from [25]. By placing the conditions $Q = 0$, $g = 0$ and $\lambda = 0$, Eq. (36) can be reduced to the transverse vibration equation of the circular plate which is not subjected to the follower force and thermal load. The first three order natural frequencies of the circular plate with three boundary conditions are calculated when the number of nodes is 13. It can be seen from Tab. 1 that the results obtained by the presented method in this paper are in a good agreement with the corresponding values from [25].

Table 1: The first four dimensionless natural frequencies of circular plate with three boundary conditions

	Boundary condition					
	Simply supported		Clamped		Free	
	this paper	[25]	this paper	[25]	this paper	[25]
ω_1	4.943	4.997	10.225	10.21	0	0
ω_2	29.774	29.76	39.811	39.78	9.023	9.084
ω_3	74.294	74.20	89.194	89.10	38.523	38.55

4.1 Circular Plate with Simply Supported Edge

Fig. 3 gives the variation of the first order dimensionless complex frequency of the circular plate with the follower force in the case of $\lambda = 1$ with variable temperature coefficient $g = -2, -1, 0, 1, 2$. It can be seen that when the follower force $Q = 0$, the dimensionless complex frequency is a real number, which indicates the natural frequency decreases with the increase of temperature coefficient g . With the increase of the follower force Q , the real part of ω becomes smaller, while the imaginary part remains zero. When the follower force Q reaches the critical value Q_c (shown in Tab. 2), the real part in the first mode becomes zero, but the imaginary part has two branches. This result shows when the follower force Q is larger than the critical load, the divergence instability appears in the first order mode of the circular plate. The reason is that the internal stress caused by the temperature change has an effect on the bending stiffness of the circular plate, which turns out the compressive stress makes the bending stiffness weaken. Meanwhile, as the average temperature of the circular plate increases with an increase of g , the natural frequency decreases.

The critical load versus the variable temperature coefficient g can be seen in Fig. 4. From Fig. 3 and Fig. 4, we can see that the temperature coefficient g increases while the first critical load decreases when the temperature load is a certain value.

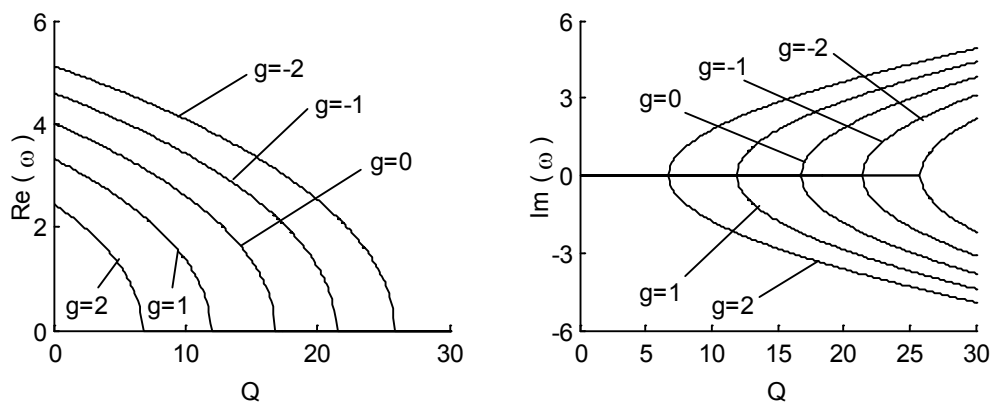


Figure 3: The first order dimensionless complex frequency versus the follower force ($\lambda = 1$)

Table 2: The first critical load of the circular plate subjected to follow force ($\lambda = 1$)

	$g_1 = -2$	$g_2 = -1$	$g_3 = 0$	$g_4 = 1$	$g_5 = 2$
Q_c	25.9	21.5	16.8	12.0	6.

Fig. 5 gives the variation of the first order dimensionless complex frequency of the circular plate with the follower force in the case of $g = 1$ and the temperature load $\lambda = 0, 1, 1.5$. As the follower force Q increases, the real part of the first order dimensionless complex frequency reduces to zero and the imaginary part appears as two branches. The circular plate appears divergence instability in the first order mode. The variation of the critical load with the temperature load λ is shown in Fig. 6. From Figs. 5 and 6, it can be seen that for a certain value of the variable temperature coefficient g , the natural frequency and the critical load decreases with the increase of the temperature load λ . With certain physical parameters and average temperature of the circular plates, the temperature load λ is mainly related to the radius-thickness ratio c , which means that with the increase of c , the first critical load decreases.

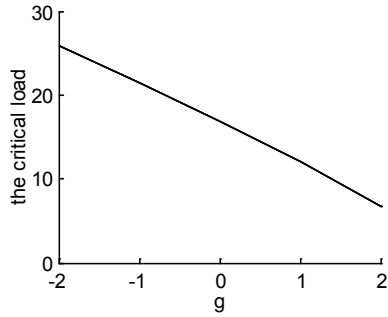


Figure 4: The critical load versus the variable temperature coefficient ($\lambda = 1$)

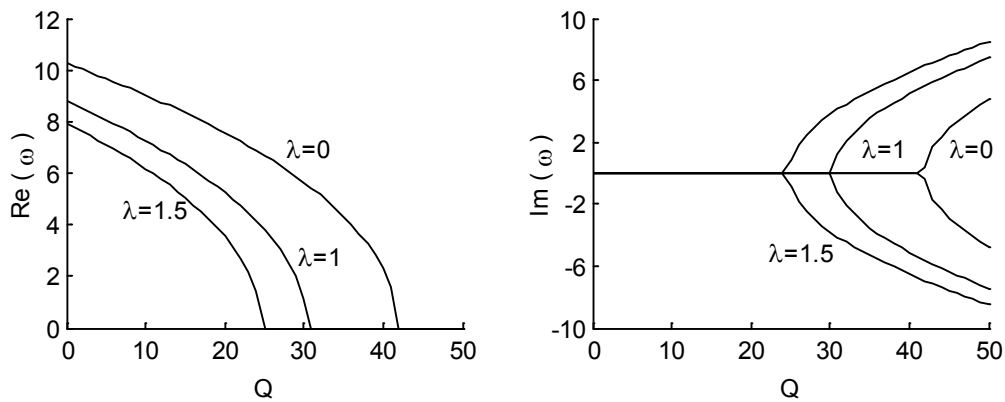


Figure 5: The first dimensionless complex frequency versus the follower force ($g = 1$)

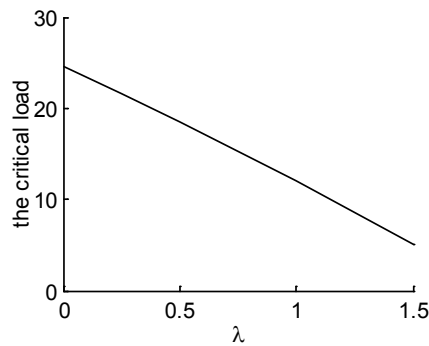


Figure 6: The critical load versus the temperature load ($g = 1$)

4.2 Circular Plate with Clamped Edge

Fig. 7 gives the variation of the first order dimensionless complex frequency of the circular plate with the follower force in the case of $\lambda = 1$ with variable temperature coefficient $g = -2, -1, 0, 1, 2$. Fig. 8 gives the variation of the first order dimensionless complex frequency of the circular plate with the follower force in the case of $g = 1$ with temperature load $\lambda = 0, 1, 1.5$. It shows that the increase of the follower force causes the real parts of ω to decrease, subsequently the imaginary parts becomes two branches, which indicates that the first order mode appears the divergence instability. This instability of the circular plate with clamped edge is similar to that with simply supported edge. Comparing Figs. 7 and 8 with Figs. 2 and 4 respectively, we can see that the change of temperature coefficient g and temperature

load λ have less effect on the complex frequency of the circular plate with the clamped edge than that with simply supported edge. The critical load with clamped edge is larger than that with simply supported edge, which shows the circular plate subjected to follow force and with clamped edge has better stability than that with simply supported edge.

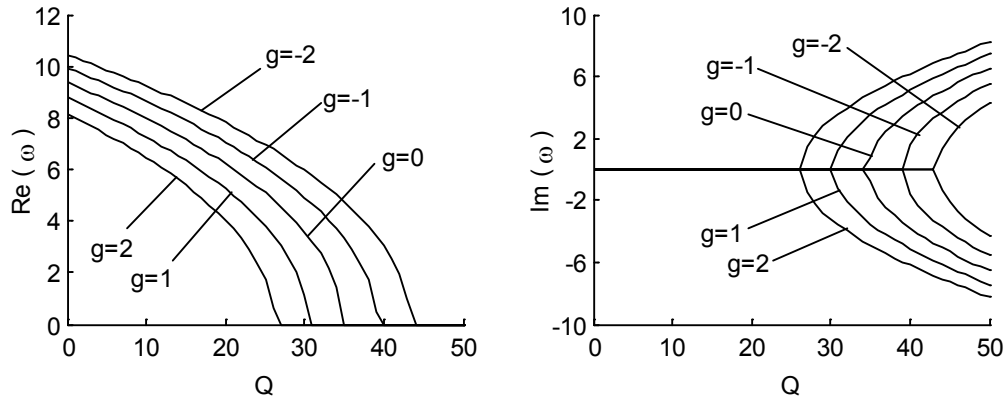


Figure 7: The first order dimensionless complex frequency versus the follower force ($\lambda = 1$)

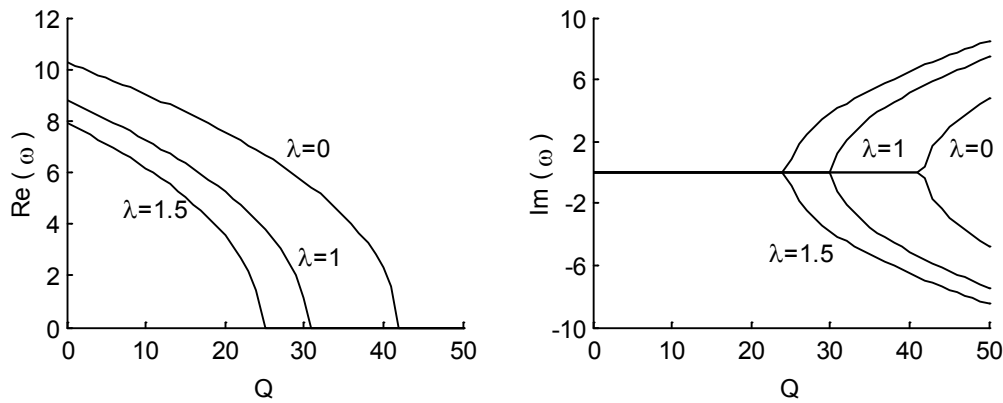


Figure 8: The first dimensionless complex frequency versus the follower force ($g = 1$)

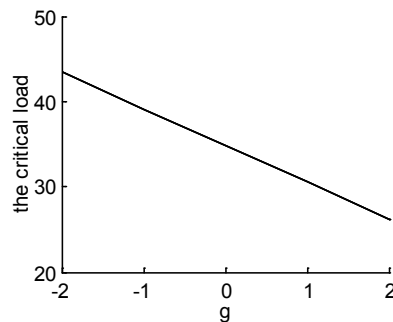


Figure 9: The critical load versus the variable temperature coefficient ($\lambda = 1$)

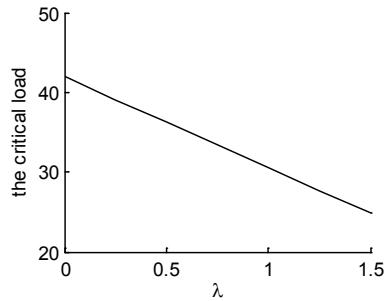


Figure 10: The critical load versus the temperature load ($g = 1$)

The variation of the critical load with the variable temperature coefficient g ($\lambda = 1$) and with the temperature load λ ($g = 1$) can be seen in Fig. 9 and Fig. 10 respectively. Comparing Figs. 9 and 10 with Figs. 4 and 6, it can be observed obviously that the critical load decreases with an increase of g and λ , which shows the critical load is not only dependent on g and λ , but also affected by the boundary condition.

4.3 Circular Plate with Free Edge

Fig. 11 shows the variation of the first order dimensionless complex frequency of the circular plate with the follower force in the case of $\lambda = 1$ and the variable temperature coefficient $g = -2, -1, 0, 1, 2$. Fig. 12 shows the variation of the first order dimensionless complex frequency of the circular plate with the follower force in the case of $g = 1$ and the temperature load $\lambda = 0, 1, 1.5$. It can be seen in Figs. 11 and 12 that the increase of the follower force leads to decrease of the real part of the first order complex frequency, and when the follower force $Q \geq Q_d$, the real parts remains zero, while the imaginary parts have two branches, which means the circular plate with free edge undergoes the divergence instability. The change of g and λ has less effect on the complex frequency of the circular plate with free edge than that with simply supported edge and clamped edge.

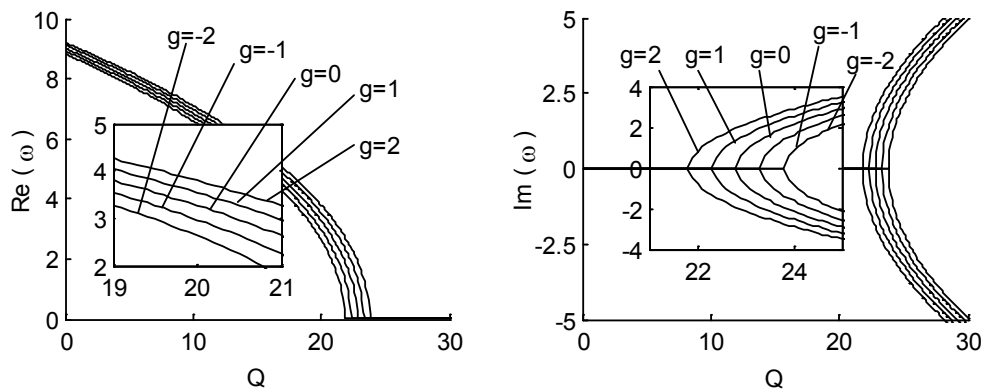


Figure 11: The first order dimensionless complex frequency versus the follower force ($\lambda = 1$)

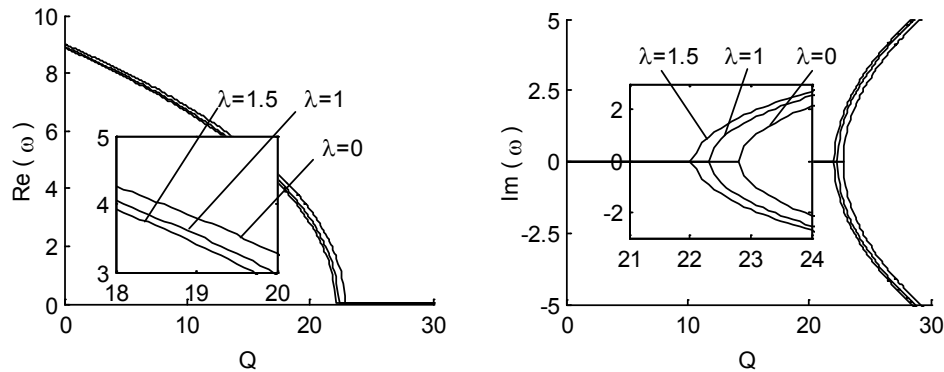


Figure 12: The first dimensionless complex frequency versus the follower force ($g = 1$)

The variation of the critical load with the variable temperature coefficient g ($\lambda = 1$) and with the temperature load λ ($g = 1$) can be seen in Fig. 13 and Fig. 14 respectively. As shown in Figs. 13 and 14, with the increase of g and λ , the critical load decreases. The critical load in the boundary condition of free edge is smaller than that in the boundary condition of clamped edge.

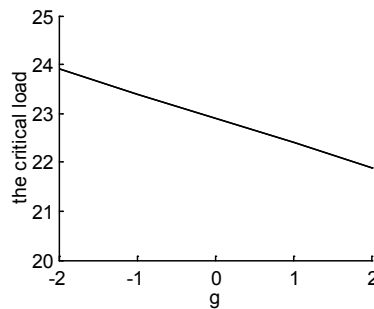


Figure 13: The critical load versus the variable temperature coefficient ($\lambda = 1$)

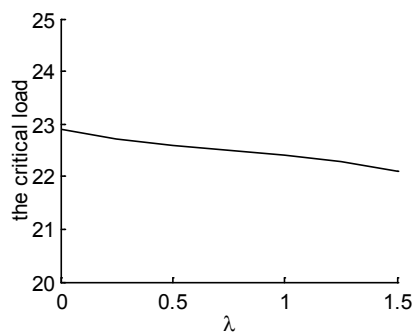


Figure 14: The critical load versus the temperature load ($g = 1$)

5 Conclusions

In this paper, the transverse vibration and stability of the circular plate subjected to follower force and thermal load with three boundaries are investigated by DQM. The effects of the follower force, the variable temperature coefficient, the temperature load and the boundary condition on transverse vibration and stability are discussed. The results are listed as follows:

(1) As the follower force increases, the real part of the first order dimensionless complex frequencies decreases to zero under all the three boundary condition, while the imaginary part has two branches with positive and negative values, which shows the circular plate subjected to follower force and thermal load undergoes divergence instability when the follower force reaches the critical load.

(2) The variable temperature coefficient and the temperature load have great effects on the natural frequency of the circular plate subjected to follower force, which are performed by the average temperature of the circular plate. As the average temperature of the circular plate increases, the natural frequency of the circular plate decreases.

(3) With an increase of the variable temperature coefficient and the temperature load, the critical load decreases under the boundary condition of simple supported edge, clamped edge and free edge. For certain conditions, the critical load of the circular plate with clamped edge is larger than that with simple supported edge and free edge, which shows that the stability of the circular plate with clamped edge is the best in the three boundary condition.

Acknowledgements: This work was supported by the National Natural Science Foundation of China (11472211); the Natural Science Foundation of Education Department of Shaanxi Province of China (2013JK1042).

References

1. Bauer, H. F., Eidel, W. (2007). Transverse vibration and stability of spinning circular plates of constant thickness and different boundary conditions. *Journal of Sound and Vibration*, 300(3-5), 877-895.
2. Khorasany, R. M. H., Hutton, S. G. (2010). An analytical study on the effect of rigid body translational degree of freedom on the vibration characteristics of elastically constrained rotating disks. *International Journal of Mechanical Sciences*, 52(9), 1186-1192.
3. Gupta, A. K., Agarwala, N., Kaurb, H. (2011). Transverse vibration of nonhomogeneous orthotropic viscoelastic circular plate of varying parabolic thickness field. *Mathematical Methods in the Applied Sciences*, 34(9), 2065-2076.
4. Wang, Z. M., Wang, Z., Zhang, R. (2014). Transverse vibration analysis of spinning circular plate based on differential quadrature method. *Journal of Vibration and Shock*, 33(1), 125-129.
5. Gupta, A. K. (2010). Vibration of nonhomogeneous Visco-Elastic circular plate of linearly varying thickness in steady state temperature field. *Journal of Theoretical and Applied Mechanics*, 48(1), 255-266.
6. Sepahi, O., Forouzan, M. R., Malekzadeh, P. (2010). Large deflection analysis of thermo-mechanical loaded annular FGM plates on nonlinear elastic foundation via DQM. *Composite Structures*, 92(10), 2369-2378.
7. Shu, X. F., Zhan, X. Q. (2000). The study of nonlinear thermoelastic free vibration of simply supported circular plate. *Engineering Mechanics*, 17(2), 97-101.
8. Sun, Y. X., Masumi, S. (2008). Vibration of microscale circular plates induced by ultra-fast lasers. *International Journal of Mechanical Sciences*, 50(9), 1365-1371.
9. Sun, Y. X., Tohmyoh, H. (2009). Thermoelastic damping of the axisymmetric vibration of circular plate resonators. *Journal of Sound and Vibrations*, 319(2), 392-405.
10. Hao, Z. L. (2008). Thermoelastic damping in the contour-mode vibrations of micro- and nano-electromechanical circular thin-plate resonators. *Journal of Sound and Vibration*, 313(1), 77-96.
11. Adali, S. (1992). Stability of a rectangular plate under nonconservative and conservative forces. *International Journal of Solids and Structures*, 18(12), 1043-1052.
12. Leipholz, H. H., Pfenndt, F. (1983). Application of extend equations of galerkin to stability problems of rectangular plates with free edges and subjected to uniformly distributed follower forces. *Computer Methods in Applied Mechanics & Engineering*, 37(3), 341-365.
13. Guo, X. X., Wang, Z. M., Wang, Y. (2011). Dynamic stability of thermoelastic coupling moving plate subjected to follower force. *International Journal of Mechanical Sciences*, 72(2), 100-107.
14. Wang, Z. M., Wang, Y., Zhou, Y. F. (2008). Dynamic stability of cracked viscoelastic rectangular plate

- subjected to follower force. *Journal of Applied Mechanics*, 75 (6).
15. Zuo, Q. H., Shreyer, H. L. (2007). Flutter and divergence instability of non-conservative beams and plates. *Journal of Sound and Vibration*, 300(3-5), 877-895.
 16. Hochlenert, D., Spelsberg-Korspete, G. R., Hagedorn, P. (2007). Friction induced vibrations in moving continua and their application to brake squeal. *Transactions of the ASME*, 74(3), 542-549.
 17. Mottershead, J. E., Chanr, S. N. (1995). Flutter instability of circular discs with frictional follower loads. *ASME Journal of Vibration and Acoustics*, 117(1), 161-163.
 18. Wang, Z. M., Gao, J. B., Li, H. X. (2003). Axially symmetric vibration and stability of circular thin plate subjected to non-conservative forces. *Chinese Journal of Solid Mechanics*, 24 (2), 155-161.
 19. Bert, C. W., Malik, M. (1997). Differential quadrature: a powerful new technique for analysis of composite structures. *Composite Structures*, 39(3-4), 179-189.
 20. Alibeigloo, A., Emtehani, A. (2015). Static and free vibration analyses of carbon nanotubereinforced composite plate using differential quadrature method. *Meccanica*, 50(1), 61-76.
 21. Han, J. B., Liew, K. M. (1997). Analysis of moderately thick circular plates using differential quadrature method. *Journal of Engineering Mechanics*, 123(12), 1247-1252.
 22. Shu, C., Chen, W. (1999). On optimal selection of interior points for applying discretized boundary conditions in DQ vibration of beams and plates. *Journal of Sound and Vibration*, 222(2), 239-257.
 23. Guo, X. X., Wang, Z. M. (2009). Analysis of the coupled thermoelastic vibration for axially moving beam. *Journal of Sound and Vibration*, 325(3), 597-608.
 24. Shao, M. H., Wu, J. M., Wu, Q. M. (2017). Vibration characteristics for moving printing membrane with variable density along the lateral direction. *Shock and Vibration*, (4), 1-10.
 25. Ni, Z. H. (1994). *Vibration mechanics*. Xi'an JiaoTong University Press.